Acta Mechanica Solida Sinica, Vol. 22, No. 1, February, 2009
Published by AMSS Press, Wuhan, China

ISSN 0894-9166

NEW STRAIN GRADIENT THEORY AND ANALYSIS**

Dake Yi **Tzu Chiang Wang*** **Shaohua Chen**

(*LNM, Institute of Mechanics, Chinese Academy of Sciences, Beijing* 100080, *China*)

Received 19 June 2008, revision received 27 October 2008

ABSTRACT A new strain gradient theory which is based on energy nonlocal model is proposed in this paper, and the theory is applied to investigate the size effects in thin metallic wire torsion, ultra-thin beam bending and micro-indentation of polycrystalline copper. First, an energy nonlocal model is suggested. Second, based on the model, a new strain gradient theory is derived. Third, the new theory is applied to analyze three representative experiments.

KEY WORDS non-local model, micro-indentation, strain gradient theory, size effect

I. INTRODUCTION

Recent years, many experiments have shown that materials display strong size effects when the characteristic length scale associated with non-uniform plastic deformation is on the order of microns. For an aluminum-silicon matrix reinforced by silicon carbide particles, Lloyd[1] observed a substantial strength increase when the particle diameter was reduced from 16 to 7.5 microns with the particle volume fraction fixed at 15%. In the experiments of measuring micro-indentation hardness of metallic materials, the square of hardness increases linearly as the depth of indentation decreases (Ma and Clarke[2]; McElhaney et al.[3]. Two direct experimental evidences that strong size effects exist have been provided by Fleck et al.[4] and Stolken and Evans[5]. The former is to measure torsion stress-strain performed on copper wires, the scaled shear strength increases by a factor 3 as the thin copper wires diameter decreases from 170 to 12 microns. The latter is to bend ultra thin beams and measure the bend moments, a significant increase in the normalized bending hardening is observed as the beam thickness decreases from 50 to 12.5 microns.

The classical plasticity theories can not predict this size dependence of material behavior at the micron scale because their constitutive models possess no internal length scale.

In order to explain the size effects, developing strain gradient theory for micron level is needed. Fleck and Hutchinson[6] proposed a phenomenological theory of strain gradient plasticity in which rotational gradient is engaged. In order to explain experimental findings of indentation (Ma and Clarke[2]; McElhaney et al.[3], fracture (Wei and Hutchinson[7]; Chen and Wang[8], Fleck and Hutchinson[9] developed strain gradient (SG) plasticity theory in which rotational gradient and stretch gradient are considered. In 1998, Nix and Gao[10] started from the Taylor relation and gave out one kind of hardening law for gradient plasticity. Motivated by the indentation hardening law, Gao et al.[11,12] proposed a mechanism-based theory of strain gradient plasticity (MSG).

* Corresponding author. Tel: +86-10-82543911(O), +86-10-82661515(H), E-mail: tcwang@imech.ac.cn

** Project supported by the National Natural Science Foundation of China (Nos. 10672165 and 10732050) and KJCX2-YW-M04.

In present paper, an energy nonlocal model is introduced in §II. Based on the model, a new strain gradient theory is proposed in §III. The theory is applied to simulate three typical experiments in §IV, §V and §VI.

II. ENERGY NONLOCAL MODEL

2.1. Classic Nonlocal Model

The classical elasticity and plasticity theories follow the local assumption that the stress at a given material point is determined only by the strain, the history of deformation and temperature at that point. However, in practice, both the nature materials and man-made materials have complicated internal structures. When the macroscopic characteristic length of the material is much larger than the internal characteristic length, the classical theories are accurate enough. Otherwise, the model needs to be enriched so as to capture the real processes more adequately.

According to the classification in Bažant[13], the non-local theories can be categorized into strongly non-local theories and weakly non-local theories. In the weakly non-local theories, the strain gradient and intrinsic length are introduced in the constitutive relations. In the strongly nonlocal theories, the local assumption is abandoned, and the stress at a given material point is determined by the strain of that point and its neighborhood. For an example, the constitutive equation of the nonlocal elasticity can be written in the form,

$$\boldsymbol{\sigma}(\boldsymbol{x}) = \int_V \boldsymbol{D}_e(\boldsymbol{x},\boldsymbol{\xi})\tilde{\boldsymbol{\varepsilon}}(\boldsymbol{\xi})\mathrm{d}\boldsymbol{\xi} = \boldsymbol{D}_e \int_V \alpha(\boldsymbol{x},\boldsymbol{\xi})\tilde{\boldsymbol{\varepsilon}}(\boldsymbol{\xi})\mathrm{d}\boldsymbol{\xi} \tag{1}$$

where V is the interaction domain, α a weight function, $\boldsymbol{D}_e$ elastic stiffness, and $\tilde{\boldsymbol{\varepsilon}}$ the local strain tensor.

For homogeneous material, we can take the weight function $\alpha(\boldsymbol{x},\boldsymbol{\xi}) = 1$ and assume $\tilde{\varepsilon}_{ij} = \varepsilon_{ij} + \varepsilon_{ij,k}\xi_k$, then we can find that the first order gradient of strain tensor $\varepsilon_{ij,k}$, has no contributions to the stress tensor, as a result, the strain gradient theory can not be derived from the nonlocal model of this type. On the other hand, the nonlocal model of this type (as shown in the Eq.(1) for the nonlocal elasticity) provides only the stress tensor and does not provide any formula for the high order stress tensor.

2.2. Energy Nonlocal Model

In the present paper, we proposed a new non-local model. In the model, the strain energy density $\tilde{w}$ at a typical point in representative volume element as shown in Fig.1, is assumed as the function of the local strain $\tilde{\varepsilon}_{ij}$ and the local rotation gradient $\tilde{\chi}_{ij}(= e_{pki}\tilde{\varepsilon}_{ij,k})$.

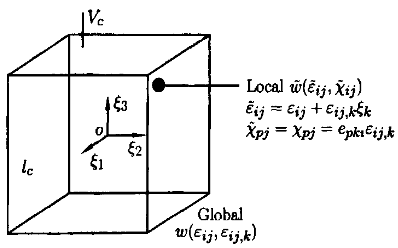

Fig. 1. The representative volume element.

The global strain energy density of the representative volume element is taken as a non-local variable as shown in Fig.1, i.e.

$$w = \frac{1}{V_c}\int_{V_c} \tilde{w}\,(\boldsymbol{X},\boldsymbol{\xi})\mathrm{d}V_c \tag{2}$$

where V_c is the volume of a representative cubic element with each boundary length l_c, $\boldsymbol{\xi}$ is the local coordinate as shown in Fig.1, with the original point at the center of cubic volume. $\boldsymbol{X}$ is the global coordinate, w is the global strain energy density and $\tilde{w}\,(\boldsymbol{X},\boldsymbol{\xi})$ is the local one.

The physical significance of l_c, which is similar to mesoscale cell size l_ε in MSG theory[10], is the boundary length of the cubic element. In MSG theory, the mesoscale cell size l_ε is in the range 10-100 nm. In the present paper, l_c is taken to be 0.1 μm order of magnitude.

The first variation of the global strain energy density w can be written as

$$\delta w = \frac{1}{V_c}\int_{V_c} \delta\tilde{w}\left(\boldsymbol{X},\boldsymbol{\xi}\right)\mathrm{d}V_c = \frac{1}{V_c}\int_{V_c} [\tilde{\sigma}_{ij}\left(\boldsymbol{X},\boldsymbol{\xi}\right)\delta\tilde{\varepsilon}_{ij}\left(\boldsymbol{X},\boldsymbol{\xi}\right) + \tilde{m}_{ij}\left(\boldsymbol{X},\boldsymbol{\xi}\right)\delta\tilde{\chi}_{ij}\left(\boldsymbol{X},\boldsymbol{\xi}\right)]\mathrm{d}V_c \tag{3}$$

where $\tilde{\sigma}_{ij}$ is the local stress tensor, $\tilde{m}_{ji}$ is the local couple stress.

If l_c is small enough, we have

$$\tilde{\varepsilon}_{ij} = \varepsilon_{ij} + \varepsilon_{ij,k}\xi_k, \quad \tilde{\chi}_{pj} = \chi_{pj} = e_{pki}\varepsilon_{ij,k} \tag{4}$$

where ε_{ij} and $\varepsilon_{ij,k}$ are the global strain and the global strain gradient respectively.

Substituting Eq.(4) into Eq.(3) yields

$$\begin{aligned}\delta w = &\frac{1}{V_c}\int_{V_c} \tilde{\sigma}_{ij}\left(\boldsymbol{X},\boldsymbol{\xi}\right)\delta\varepsilon_{ij}\left(\boldsymbol{X}\right)\mathrm{d}V_c + \frac{1}{V_c}\int_{V_c} \tilde{\sigma}_{ij}\left(\boldsymbol{X},\boldsymbol{\xi}\right)\delta\varepsilon_{ij,k}\left(\boldsymbol{X}\right)\xi_k\mathrm{d}V_c \\ &+\frac{1}{V_c}\int_{V_c} \tilde{m}_{pj}\left(\boldsymbol{X},\boldsymbol{\xi}\right)e_{pki}\delta\varepsilon_{ij,k}\left(\boldsymbol{X}\right)\mathrm{d}V_c = \sigma_{ij}\delta\varepsilon_{ij} + \tau_{ijk}\delta\varepsilon_{ij,k}\end{aligned} \tag{5}$$

Then we have

$$\sigma_{ij} = \frac{\partial w}{\partial \varepsilon_{ij}} \tag{6}$$

$$\tau_{ijk} = \frac{1}{2}\left(\frac{\partial w}{\partial \varepsilon_{ij,k}} + \frac{\partial w}{\partial \varepsilon_{ji,k}}\right) \tag{7}$$

III. NEW STRAIN GRADIENT THEORY

3.1. Equilibrium Equations and Boundary Conditions

The first variation of total potential energy Π can be written as

$$\begin{aligned}\delta\Pi &= \int_V \delta w\mathrm{d}V - \int_V f_i\delta u_i\mathrm{d}V - \int_S \bar{p}_i\delta u_i\mathrm{d}S - \int_S \bar{r}_i D\delta u_i\mathrm{d}S \\ &= \int_V (\sigma_{ij}\delta\varepsilon_{ij} + \tau_{ijk}\delta\varepsilon_{ij,k})\mathrm{d}V - \int_V f_i\delta u_i\mathrm{d}V - \int_S \bar{p}_i\delta u_i\mathrm{d}S - \int_S \bar{r}_i D\delta u_i\mathrm{d}S\end{aligned} \tag{8}$$

where V is the volume, S the boundary of V, f_i the force per unit volume, and u_i the displacement. $D = \boldsymbol{n}\cdot\nabla$, $\boldsymbol{n}$ is the unit outward normal to S, and ∇ is the spatial gradient operator. $\bar{p}_i$ and $\bar{r}_i$ are generalized surface tractions.

According minimum total potential energy principle, we can obtain equilibrium equations

$$\left(\sigma_{ij} - \tau_{ijk,k}\right)_{,j} + f_i = 0 \qquad \text{in} \quad V \tag{9}$$

and boundary conditions

$$\left(\sigma_{ij} - \tau_{ijk,k} + \left(\bar{\partial}_p n_p\right)\tau_{ijk}n_k\right)n_j - \bar{\partial}_j\tau_{ijk}n_k = \bar{p}_i \qquad \text{on} \quad S_\sigma \tag{10a}$$

$$u_i = \bar{u}_i \qquad \text{on} \quad S_u \tag{10b}$$

$$n_j n_k \tau_{ijk} = \bar{r}_i \qquad \text{on} \quad S_\tau \tag{11a}$$

$$Du_i = D\bar{u}_i \qquad \text{on} \quad S_{Du} \tag{11b}$$

3.2. Constitutive Equation for Power Law Hardening Materials

According to Fleck and Hutchinson[9], the local strain energy-density is assumed to be the function of a local generalized effective strain $\tilde{E}_e$ and written as

$$\tilde{w} = \int_0^{\tilde{E}_e} \tilde{\Sigma}_e \mathrm{d}\tilde{E}_e + \frac{1}{2}K\tilde{\varepsilon}_v^2 = \int_0^{\tilde{E}_e} \sigma_Y \left(\frac{\tilde{E}_e}{\varepsilon_Y}\right)^n \mathrm{d}\tilde{E}_e + \frac{1}{2}K\tilde{\varepsilon}_v^2 = \frac{\sigma_Y \varepsilon_Y}{1+n}\left(\frac{\tilde{E}_e}{\varepsilon_Y}\right)^{1+n} + \frac{1}{2}K\tilde{\varepsilon}_v^2 \tag{12}$$

where $\tilde{\Sigma}_e$ is local generalized effective stress.

The local strain energy density $\tilde{w}$ can be approximately expressed as

$$\tilde{w} = w^0 + w^0_{,k}\xi_k + \frac{w^0_{,kl}}{2}\xi_k\xi_l \qquad \text{on} \quad V_c \tag{13}$$

where

$$w^0 = (\tilde{w})_{\xi=0} = \frac{\sigma_Y \varepsilon_Y}{1+n}\left(\frac{E_e}{\varepsilon_Y}\right)^{1+n} + \frac{1}{2}K\varepsilon_v^2 \tag{14}$$

$$w^0_{,kl} = (\tilde{w}_{,kl})_{\xi=0} = \frac{2\sigma_Y}{3(\varepsilon_Y)^n}\left[\frac{2(n-1)(E_e)^{n-3}\varepsilon'_{mn}\varepsilon'_{mn,k}\varepsilon'_{ij}\varepsilon'_{ij,l}}{3} + (E_e)^{n-1}\varepsilon'_{ij,l}\varepsilon'_{ij,k}\right] + K\varepsilon_{v,l}\varepsilon_{v,k} \tag{15}$$

Substituting Eq.(13) into Eq.(2) yields

$$w = \frac{1}{V_c}\int_{V_c}\left(w^0 + w^0_{,k}\xi_k + \frac{w^0_{,kl}}{2}\xi_k\xi_l\right)\mathrm{d}V_c = w^0 + A_k w^0_{,k} + B_{kl}w^0_{,kl} \tag{16}$$

where

$$A_k = \frac{1}{V_c}\int_{V_c}\xi_k \mathrm{d}V_c, \quad B_{kl} = \frac{1}{2V_c}\int_{V_c}\xi_k\xi_l \mathrm{d}V_c \tag{17}$$

ξ_k is an anti-symmetric function in V_c about center of cubic region, then

$$A_k = 0, \quad B_{kl} = B\delta_{kl} = \frac{1}{2V_c}\int_{V_c}(\xi_1)^2 \mathrm{d}V_c\delta_{kl} = \frac{l_c^2}{24}\delta_{kl} \tag{18}$$

$$w = w^0 + B_{kl}w^0_{,kl} \tag{19}$$

According work conjugate relation, the global stress σ_{ij} and high order stress τ_{ijk} can be written very easily as

$$\begin{aligned}\sigma_{ij} = \frac{\partial w}{\partial \varepsilon_{ij}} &= \frac{2\sigma_Y}{3(\varepsilon_Y)^n}(E_e)^{n-1}\varepsilon'_{ij} + K\varepsilon_v\delta_{ij} \\ &+ \frac{4\sigma_Y(n-1)B}{9(\varepsilon_Y)^n}\left[\frac{2(n-3)(E_e)^{n-5}\varepsilon'_{mn}\varepsilon'_{mn,k}\varepsilon'_{pq}\varepsilon'_{pq,k}}{3} + (E_e)^{n-3}\varepsilon'_{mn,k}\varepsilon'_{mn,k}\right]\varepsilon'_{ij} \\ &+ \frac{8(n-1)B\sigma_Y}{9(\varepsilon_Y)^n}(E_e)^{n-3}\varepsilon'_{mn}\varepsilon'_{mn,k}\varepsilon'_{ij,k}\end{aligned} \tag{20}$$

and

$$\begin{aligned}\tau_{ijk} = \frac{1}{2}\left(\frac{\partial w}{\partial \varepsilon_{ij,k}} + \frac{\partial w}{\partial \varepsilon_{ji,k}}\right) &= \frac{4\sigma_Y B(E_e)^{n-1}}{3(\varepsilon_Y)^n}\varepsilon'_{ij,k} + \frac{8\sigma_Y B(n-1)(E_e)^{n-3}\varepsilon'_{ij}\varepsilon'_{mn}\varepsilon'_{mn,k}}{9(\varepsilon_Y)^n} \\ &+ \frac{l_{cs}^2\sigma_Y}{3(\varepsilon_Y)^n}\left[(E_e)^{n-1} + \frac{4B(n-1)(n-3)(E_e)^{n-5}\varepsilon'_{mn}\varepsilon'_{mn,r}\varepsilon'_{st}\varepsilon'_{st,r}}{9}\right. \\ &\left. + \frac{2B(n-1)(E_e)^{n-3}\varepsilon'_{mn,l}\varepsilon'_{mn,l}}{3}\right](e_{pki}\chi_{pj} + e_{pkj}\chi_{pi}) + 2BK\varepsilon_{v,k}\delta_{ij}\end{aligned} \tag{21}$$

IV. THIN WIRE TORSION

The size effects emerging in the experiment of thin-wire torsion[4] is analyzed using the present strain gradient theory. A Cartesian coordinate system (x_1, x_2, x_3) and a cylindrical polar coordinate system (r, θ, x_3) are introduced. The radius of the wire denotes as a, and κ is the twist per unit length of the wire.

The displacement fields

$$u_1 = -\kappa x_2 x_3, \quad u_2 = \kappa x_1 x_3, \quad u_3 = 0 \tag{22}$$

lead to the non-vanishing strain components, strain gradient and rotation gradient components as

$$\varepsilon_{13} = \varepsilon_{31} = -\frac{1}{2}\kappa x_2, \quad \varepsilon_{23} = \varepsilon_{32} = \frac{1}{2}\kappa x_1 \tag{23}$$

$$\varepsilon_{13,2} = \varepsilon_{31,2} = -\frac{1}{2}\kappa, \quad \varepsilon_{23,1} = \varepsilon_{32,1} = \frac{1}{2}\kappa \tag{24}$$

$$\chi_{11} = \chi_{22} = -\frac{1}{2}\kappa, \quad \chi_{33} = \kappa \tag{25}$$

The total strain energy for a unit length of the bar is given by

$$\begin{aligned} W &= \int_V w \mathrm{d}V = \int_V \left(w^0 + B_{kl} w^0_{,kl}\right) \mathrm{d}V = \int_0^\kappa Q(\kappa) \mathrm{d}\kappa \\ &= \frac{2\pi\sigma_Y}{(1+n)(3+n)\varepsilon_Y^n}\left(\frac{1}{3}\right)^{(1+n)/2} \kappa^{1+n}\left[\left(a^2+3l_{cs}^2\right)^{(n+3)/2} - \left(3l_{cs}^2\right)^{(n+3)/2}\right] \\ &\quad + \frac{4\pi B\sigma_Y \kappa^{n+1}}{3^{(n+1)/2}(\varepsilon_Y)^n}\left[\frac{\left(a^2+3l_{cs}^2\right)^{(n+1)/2}}{2} - \frac{3l_{cs}^2}{2}\left(a^2+3l_{cs}^2\right)^{(n-1)/2}\right] \end{aligned} \tag{26}$$

Let $\beta = 3l_{cs}^2/a^2$, the torque Q can be written as

$$Q = \frac{\mathrm{d}W}{\mathrm{d}\kappa} = \frac{2\pi\sigma_Y \kappa^n a^{n+3}}{(n+3)\varepsilon_Y^n 3^{(1+n)/2}}\left\{\left[(1+\beta)^{(n+3)/2} - \beta^{(n+3)/2}\right] + \frac{B(1+n)(3+n)}{a^2}(1+\beta)^{(n-1)/2}\right\} \tag{27}$$

When $l_c/a << 1$, $l_{cs}/a << 1$, Eq.(27) can be simplified as

$$\frac{Q}{a^3} = \frac{2\pi\sigma_Y}{(3+n)\varepsilon_Y^n}(\kappa a)^n\left(\frac{1}{3}\right)^{(1+n)/2} \tag{28}$$

Since the intrinsic lengths l_{cs} and l_c are much smaller than 170 μm, we choose the torque experiment results of the thin-wire with diameter $2a = 170\ \mu$m as a calibration curve and obtain $\frac{2\pi\sigma_Y}{(3+n)\varepsilon_Y^n}\left(\frac{1}{3}\right)^{(1+n)/2} =$ 232.7 MPa, $n = 0.21$, which is close to the tensile experimental results given by Fleck et al.[4].

According to Gao et al.[11] and Fleck et al.[4], we take $l_c = 0.1\ \mu$m and $l_{cs} = 3.7\ \mu$m . The theoretical results compared with the experiment ones are shown in Fig.2. One can see both are consistent very well with each other.

V. ULTRA-THIN BEAM BEND

Now, we study the problem of Ultra-thin beam bending with different micro-meters thickness using the present strain gradient theory. A Cartesian coordinate system (x_1, x_2, x_3) is introduced. h is the thickness of beams, b the width and κ the curvature.

The displacement fields

$$u_1 = \kappa x_1 x_2, \quad u_2 = \kappa\frac{\left(x_1^2 + x_2^2\right)}{2}, \quad u_3 = 0 \tag{29}$$

lead to the non-vanishing strain components, strain gradient and rotation gradient components as follows:

$$\varepsilon_{11} = -\varepsilon_{22} = \kappa x_2, \quad \varepsilon_{11,2} = -\varepsilon_{22,2} = \kappa, \quad \chi_{31} = -\kappa \tag{30}$$

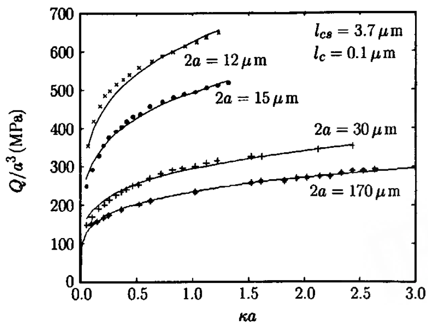

Fig. 2. Plots of torque against the surface strain for copper wires with different diameters. The solid lines denote the present theoretical results and the dotted lines denote the experiment ones[4].

Following Stölken and Evans[5], neglecting the elastic deformation, the relation between the local generalized effective stress and the local generalized effective strain can be expressed as

$$\tilde{\Sigma}_e = \frac{\sqrt{3}}{2}\Sigma_0 + \frac{3}{4}E_p\tilde{E}_e \tag{31}$$

where Σ_0 is the yield strength, E_p is the hardening coefficient.

The total strain energy per unit length is given by

$$W = \int_V (w^0 + B_{kl}w^0_{,kl})\,\mathrm{d}V = 2b\kappa\Sigma_0\left[\frac{h}{4}\sqrt{\frac{h^2}{4}+\frac{l_{cs}^2}{2}}+\frac{l_{cs}^2}{4}\ln\left(\frac{h}{\sqrt{2}l_{cs}}+\sqrt{\frac{h^2}{2l_{cs}^2}+1}\right)\right]$$

$$+2b\left(\frac{1}{48}E_p\kappa^2h^3+\frac{B\Sigma_0\kappa h}{\sqrt{h^2+2l_{cs}^2}}+BE_p\kappa^2\frac{h^2}{+}E_p\kappa^2\frac{l_{cs}^2}{8}h\right) \tag{32}$$

Substituting Eq.(32) into

$$M = \frac{\mathrm{d}W}{d\kappa} \tag{33}$$

yields the non-dimensional bending moment

$$\frac{4M}{bh^2\Sigma_0} = \sqrt{1+\frac{2l_{cs}^2}{h^2}}+\frac{2l_{cs}^2}{h^2}\ln\left(\frac{h}{\sqrt{2}l_{cs}}+\sqrt{\frac{h^2}{2l_{cs}^2}+1}\right)$$

$$+\frac{8B}{h^2\sqrt{1+2l_{cs}^2/h^2}}+\frac{2}{3\Sigma_0}E_p\varepsilon_b+\frac{16BE_p\varepsilon_b}{h^2\Sigma_0}+\frac{4E_pl_{cs}^2\varepsilon_b}{h^2\Sigma_0} \tag{34}$$

where $\varepsilon_b = h\kappa/2$ is surface plastic strain.

The yield strength Σ_0 and the hardening coefficient E_p with different thicknesses were measured by Stölken and Evans[5]. We take $l_c = 0.1\,\mu$m and fit the experiment results given by Stölken and Evans[5] with Eq.(34). The comparison among the present results, SG theory results (Fleck and Hutchinson[9]) and the experiment ones is shown in Fig.3. From Fig.3, one can find the two theoretical results are close and agree with the experiment results. In the present theory, intrinsic length for rotation gradient $l_{cs}(= 5.8\,\mu$ m), which lies in a micro-meter range, agrees with the result in Stölken and Evans[5] (intrinsic length for rotation gradient $l_R = 5\,\mu$m) and the result in Chen and Wang[14] (intrinsic length for rotation gradient $l_R = 7\,\mu$m).

VI. ANALYSIS OF MICRO-INDENTATION

6.1. Indentation Model

The indenter is assumed to be axisymmetric and conical. The half-angle of the indenter, $\beta = 72°$. The indenter is assumed to be frictionless. The depth of indentation is δ, the contact radius of indentation

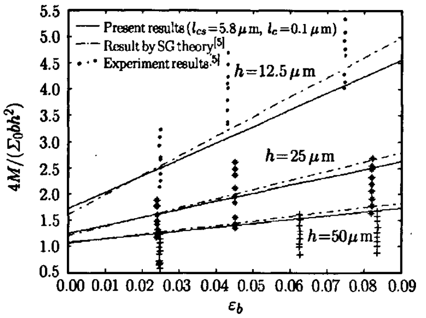

Fig. 3. Plots of bending moment against the surface strain for three beams with different thickness.

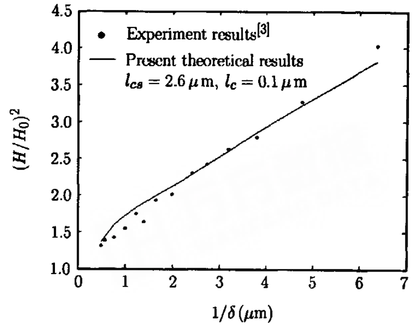

Fig. 4. Comparison of $(H/H_0)^2$ with the inverse of indentation depth, $1/\delta$.

is a, and the contact depth $h = a/\tan\beta$. The total force, P, exerted on the indenter is the sum of nodal forces in the z-direction for those nodes in contact with the indenter .The indentation hardness is defined as

$$H = \frac{|P|}{\pi a^2} \tag{35}$$

The displacement boundary conditions can be written as

$$(u_r)_{r=0} = 0 \tag{36}$$

$$(u_z)_{z=0} = 0 \tag{37}$$

and

$$u_z(r) = -\delta + \frac{r}{\tan\beta}, \qquad 0 \le r \le a \quad \text{on the contacted surface} \tag{38}$$

The force boundary conditions can be written as

$$\bar{p}_z = 0 \quad (r > a) \tag{39}$$

$$\bar{p}_r = 0 \quad (r > 0) \tag{40}$$

and

$$\bar{r}_z = \bar{r}_r = 0 \quad (r \ge 0) \tag{41}$$

where $\bar{p}$ is the surface traction, and $\bar{r}$ is the higher order surface traction.

6.2. Calculation Results

Referring to Qiu[15], the elastic modulus, Poisson's ratio, reference stress and the plastic hardening exponent of the polycrystalline copper are E = 109.2 GPa, ν = 0.3, $\sigma_{\rm ref}$ = 688 MPa, and N = 0.3, respectively.

The stress-strain law of copper in uniaxial tension is shown as

$$\sigma = \begin{cases} E\varepsilon_x & (\varepsilon \le \sigma_Y/E) \\ \sigma_{\rm ref}\varepsilon_x^N & (\varepsilon > \sigma_Y/E) \end{cases} \tag{42}$$

From Fig.4, one can clearly see that the linear relation between the square of indentation hardness, H^2, and the inverse of indentation depth, $1/\delta$, exists when the indentation depth δ is less than 1 μm.

VII. SUMMARY

A new framework of non-local model is proposed, in which the strain energy density of a representative volume element is taken as a non-local variable. Based on the non-local model, a new strain gradient theory is derived. Compared with existing gradient theories, the present one has a clearer physical background.

Size effects in three typical experiments, i.e., the thin wire torsion, the micro-beam bending and the micro indentation of polycrystalline copper, have been analyzed using the present strain gradient theory. It is found that the results predicted by the present theoretical model are consistent well with the experimental ones.

References

[1] Lloyd,D.J., Particle reinforced aluminum and magnesium metal matrix composites. *International Materials Reviews*, 1994, 39(1): 1-45.

[2] Ma,Q., and Clarke,D.R., Size dependent hardness of silver single crystals. *Journal of Materials Research*, 1995, 10(4): 853-863.

[3] McElhaney,K.W., Vlassak,J.J. and Nix,W.D., Determination of indenter tip geometry and indentation contact area for depth-sening indentation experiments, *Journal of Materials Research*, 1998, 13(5): 1300-1306.

[4] Fleck,N.A., Muller,G.M., Ashby,M.F. and Hutchinson.J.W., Strain gradient plasticity: theory and experiment. *Acta Metallurgica et Materialia*, 1994, 42(2), 475-487.

[5] Stölken,J.S. and Evans,A.G., A microbend test method for measuring the plasticity length scale, *Acta Materialia*, 1998, 46(14): 5109-5115.

[6] Fleck,N.A. and Hutchinson,J.W., A phenomenological theory for strain gradient effects in plasticity. *Journal of the Mechanics and Physics of Solids*, 1993, 41(12): 1825-1857.

[7] Wei,Y.G. and Hutchinson,J.W., Steady-state crack growth and work of fracture for solids characterized by strain gradient plasticity. *Journal of the Mechanics and Physics of Solids*, 1997, 45(8): 1253-1273.

[8] Chen,S.H. and Wang,T.C., Finite element solutions for plane strain mode I crack with strain gradient effects. *International Journal of Solids and Structures*, 2002, 39(5): 1241-1257.

[9] Fleck,N.A. and Hutchinson,J.W., Strain Gradient Plasticity. *Advances in Applied Mechanics*, 1997, 33: 295-361.

[10] Nix,W.D. and Gao,H., Indentation size effects in crystalline materials: a law for strain plasticity. *Journal of the Mechanics and Physics of Solids*, 1998, 46(3): 411-425.

[11] Gao,H., Huang,Y., Nix,W.D. and Hutchinson,J.W., Mechanism-based strain gradient plasticity — I. Theory. *Journal of the Mechanics and Physics of Solids*, 1999, 47(6): 1239-1263.

[12] Gao,H., Huang,Y., Nix,W.D. and Hutchinson,J.W., Mechanism-based strain gradient plasticity — II. Analysis. *Journal of the Mechanics and Physics of Solids*, 2000, 48(1): 99-128.

[13] Bažant,Z.P. and Milan,Jirasek., Nonlocal integral formulations of plasticity and damage: survey of progress. *Journal of Engineering Mechanics*, 2002, 128(11): 1119-1149.

[14] Chen,S.H and Wang,T.C., Strain gradient theory with couple stress for crystalline solids. *European Journal of Mechanics A-Solids*, 2001, 20(5): 739-756.

[15] Qiu,X.M., Development and Applications of Mechanism Based Strain Gradient Plasticity. Doctor thesis. Beijing: Tsinghua University, 2001 (in Chinese).